Optics & Laser Technology 54 (2013) 401–406

Contents lists available at SciVerse ScienceDirect

Optics & Laser Technology

journal homepage: www.elsevier.com/locate/optlastec

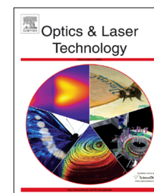

Enhanced spectrum superluminescent diodes fabricated by infrared laser rapid thermal annealing

Romain Beal, Khalid Moumanis, Vincent Aimez, Jan J. Dubowski *

Laboratory for Quantum Semiconductors and Photon-based BioNanotechnology, Interdisciplinary Institute for Technological Innovation (3IT), Université de Sherbrooke, 3000, boulevard de l'Université Sherbrooke, Québec, J1K 0A5, Canada

ARTICLE INFO

Article history:
Received 2 April 2013
Received in revised form
25 June 2013
Accepted 28 June 2013

Keywords:
Superluminescent diodes
Quantum well intermixing
Laser annealing

ABSTRACT

We report on the fabrication of superluminescent diodes (SLD) from a graded bandgap quantum well intermixed (QWI) material obtained by an infrared laser rapid thermal annealing (IR Laser-RTA) technique. The processed semiconductor wafer consisted of an InGaAs/InGaAsP/InP (001) QW laser heterostructure originally emitting at 1.55 μm. The combined beams of a 150 W laser diode operating at 980 nm and a 30 W Nd:YAG laser operating at 1064 nm are used to heat the sample. While the laser diode is used for back-side heating of the wafer, the Nd:YAG laser beam is swept along the sample surface, resulting in temperature gradient changing in the direction perpendicular to the scan. This contactless RTA approach, allowed to obtain a graded bandgap material that was employed for the fabrication of SLD devices with a broadened emission bandwidth. The lasing effect in a series of 3 mm long broad area injection diodes was suppressed by tilting their facets by 7.5° with respect to the [110] direction. The best SLD devices had their FWHM (full-width-at-half-maximum) emission increased by 33% in comparison to the FWHM of 36 nm observed for devices made from the as grown material at an equal output power of 0.8 mW.

© 2013 Elsevier Ltd. All rights reserved.

1. Introduction

Superluminescent diodes (SLDs), due to their broad emission spectrum, find applications in optical coherence tomography, e.g. for cornea and retina diagnostics [1], optoelectronic components testing (transmission/reflection spectra, dispersion), fiber-optic sensors (temperature, strain or pressure measurements) and fiber-optic gyroscopes [2]. For these applications, SLDs with broad-band optical spectra and high intensity emission are desirable. Indeed, optical coherent tomography sees its resolution increase with spectral bandwidth, and high output power offers a better signal-to-noise ratio. For fiber optic based sensors, SLD short coherence length allows feedback and mode partition noise reduction compared to a laser-based system [3]. A typical SLD structure is similar to that of a laser diode p–n junction containing a quantum well (QW) or quantum dot (QD) active region and an optical waveguide. Broad area emission of SLDs is achieved by suppressing Fabry–Perot resonance induced by reflections from optical waveguide facets. Facet reflections can be reduced by using tilted facets [4,5], J-shaped waveguide [6], absorption region on device rear side [7], or anti-reflecting coatings [8]. Current commercial devices offer output power from tenths of a milliwatt to several tens of milliwatts, depending on desired central wavelength and spectral width [9].

To increase SLDs' spectral width, different approaches have been studied. The common method is to increase the active region gain spectrum by using chirped QWs [10] or self-assembled QDs that exhibit broad emission due to their natural size distribution [11–13]. In some cases, independent electrodes are used along the waveguide in order to obtain the combined contribution of ground and excited states emission to the emitted spectrum [14–16]. Other approaches take advantage of the bandgap variation in light emission direction; this has been realized by selective area epitaxy [17] and by multi step epitaxy [18]. However, as the repeatability of epitaxial techniques remains to be a challenging problem, the growth of multi wavelength structures is not a straightforward process.

To avoid the epitaxial growth related issues, post-growth quantum well intermixing (QWI) has been investigated for the fabrication of SLDs. Thereby, the use of ion implantation induced disordering (IIID) produced devices emitting 1.7 mW power at a 95 nm spectral width, compared to a 45 nm for the as-grown material made devices [19]. A 130% increase of the spectral width was also reported for a high power device comprising SLD and a semiconductor optical amplifier (210 mW for a 37 nm spectral

* Corresponding author. Tel.: +1 819 8218000 62528.
E-mail addresses: romain.beal@usherbrooke.ca (R. Beal), khalid.moumanis@usherbrooke.ca (K. Moumanis), vincent.aimez@usherbrooke.ca (V. Aimez), jan.j.dubowski@usherbrooke.ca (J.J. Dubowski).
URL: http://www.dubowski.ca (J.J. Dubowski).

0030-3992/$ - see front matter © 2013 Elsevier Ltd. All rights reserved.
http://dx.doi.org/10.1016/j.optlastec.2013.06.032

width) [20] that was obtained by impurity free vacancy disordering (IFVD). More recently, FWHM over 300 nm at 1145 nm center wavelength was obtained at milliwatt power level by using IFVD in InAs/InGaAs/GaAs dot-in-well structures [21]. Both IFVD and IIID techniques become relatively complex and time consuming when used for delivering structures with several degrees of intermixing. This complexity arises from the need of a grayscale mask for IIID and multiple material and/or thickness deposition on selected regions of wafers for IFVD. In contrast, laser induced QWI offers a possibility of contactless processing at selected regions of semiconductor wafers, without the need of complex mask deposition. Early experiments of IR laser annealing and QWI, referred to as photo-absorption induced disordering [22], allowed to observe an increase in FWHM of InGaAs-InAlGaAs-based device emission from 125 nm to over 260 nm. However, besides the very low output power level achieved (less than 0.1 mW), this process was limited to a single annealed spot (the laser beam and the sample being motionless during the experiment), which makes it inappropriate for efficient device mass production. More recently, similar experiments were conducted on QD microstructures, still using a single laser beam combined with a hot plate providing background heating [23]. Devices were intermixed after fabrication, as openings in the metal contact pad helped define the regions to be intermixed. This offers the advantage of limiting the annealing area, thereby limiting the annealing time. However, these processing methods seem not suitable for mass scale production and the use of a metal pad as a mask could limit the flexibility of the process.

We have investigated infrared laser rapid thermal annealing for QD intermixing [24] and fabrication of multi wavelength laser arrays emitting in the 1400–1525 nm range [25]. Recently, we developed a 2-IR Laser-RTA technique that could be used, without the need of a dedicated mask and/or an etching procedure, to deliver selective-area processed material with arbitrary contour regions [26]. We have also demonstrated that the IR Laser-RTA technique can be used for precise tuning of emission wavelength at small sites (~280 μm in diameter) of QW wafers [27]. In addition to the spatial control of the laser beam position, the control of laser beam scanning speed allows controlling its dwell time and, thus, the annealing conditions along the path defined by laser spots. Furthermore, thanks to the innovative simultaneous use of two IR lasers, the high power beam damage that can be caused by a single laser beam irradiation has been significantly reduced. Here, we examine this seemingly promising approach application to the fabrication of QW wafers with almost arbitrary gradients of bandgap shifted material and report on the operation SLD fabricated from this material; thus having its spectral width performances improved in comparison to as grown material.

2. Experimental details

2.1. Material

We used a five QWs InGaAs/InGaAsP laser heterostructure grown on an n-InP substrate by metalorganic Chemical Vapour Deposition (MOCVD). The thickness and composition of the QWs was designed to have a material emitting at 1.5 μm at room temperature. The details of the heterostructure are shown in Fig. 1. An 18.5 nm thick cap of SiO_2 was deposited by plasma-enhanced CVD on top of the microstructure to protect its surface from deterioration during high-temperature annealing. The relatively thin cap was chosen in this case to minimize the error of the QWI temperature measured with an optical pyrometer. Additionally, a 400 nm-thick sacrificial layer of undoped InP was added during the epitaxial growth of the heterostructure to protect the InGaAs contact layer. Following the annealing step, both the SiO_2 and sacrificial layers were etched away to provide a high quality defect-free surface for electrical contacts. The bottom of the microstructure was protected during the annealing with a 266 nm thick SiO_2 cap. This cap was also etched away to allow for electrical contacting to the substrate.

Layer	
400 nm InP **sacrificial layer** U/D	
100 nm InGaAs **etch stop** p^+ Zn 8 x 10^{18} cm^{-3}	
50 nm InGaAsP 1.2Q p^+ Zn 2 x 10^{18} cm^{-3}	
1200 nm InP **upper cladding** p^+ Zn 6 x 10^{17} cm^{-3}	
10 nm 1.3Q InGaAsP **etch stop** p^+ Zn 6 x 10^{17} cm^{-3}	
200 nm InP p^+ Zn 6 x 10^{17} cm^{-3}	
80 nm InGaAsP 1.05Q **upper waveguiding core** n^+ Si 5 x 10^{17} cm^{-3}	
50 nm InGaAsP 1.2Q n^+ Si 5 x 10^{17} cm^{-3}	
12 nm InGaAsP **barrier** 1.25Q U/D	
5 nm InGaAs **quantum well** U/D	X 5
12 nm InGaAsP **barrier** 1.25Q U/D	
50 nm InGaAsP 1.2Q n^+ Si 5 x 10^{17} cm^{-3}	
80 nm InGaAsP 1.05Q **lower waveguiding core** n^+ Si 5 x 10^{17} cm^{-3}	
1400 nm InP **lower cladding** n^+ Si 2 x 10^{18} cm^{-3}	
InP **substrate** n^+ S 2 x 10^{18} cm^{-3}	

Fig. 1. Cross-sectional view of the InGaAs/InGaAsP/InP QW heterostructure employed in this study.

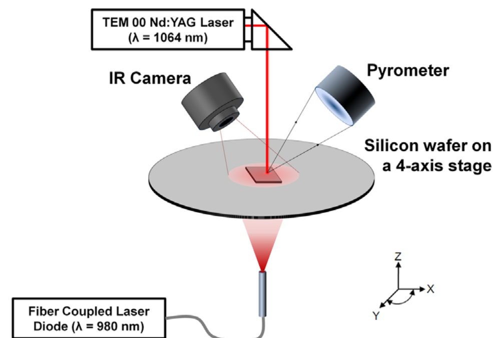

Fig. 2. Schematic of the IR Laser RTA setup.

2.2. IR Laser-RTA setup

The experimental set up, as illustrated in Fig. 2, is based on the combined use of a 980 nm CW GaAs/AlGaAs laser diode (LD) Apollo Instruments Inc., Irvine, CA and a 1064 nm TEM00 Nd:YAG CW laser (Quantronix, Santa Clara, CA) as previously reported [26,27]. The pigtailed fiber (1 mm core, Numerical Aperture = 0.22) coupled with the LD is used to deliver power of up to 150 W to the back of a 2" silicon wafer. This wafer remained in contact with the InP substrate of processed InGaAs/InGaAsP samples. The LD, operating at 30 W, projected a 10 mm diameter spot on the Si wafer, resulting in background heating of almost the entire sample. The front side of the sample was irradiated with 500 μm diameter spot of the Nd:YAG laser, set to deliver 450 mW of power. The Nd:YAG laser beam scanned the sample surface by means of a galvanometric rastering system at a 200 mm/s. For 10,000 iterations (one iteration being a two-way scan) over the 1.8 mm long scan, the total processing (annealing) time was approximately 200 s per one line. A total of 8 lines were processed over the sample surface, in two parallel series of 4 lines separated by 400 μm. The in-situ temperature measurements were carried

out using a 2-channel fiber optic Micron M680 pyrometer and a custom made IR camera (IR-CAM). The pyrometer allowed the collection of radiation from circular areas of 0.45 and 0.7 mm in diameter while the IR-CAM, equipped with 820–840 nm bandpass filter, was used to monitor the sample temperature in the center of processed lines. The LD output power was controlled in a feed-back loop to maintain the maximum sample temperature at 690 °C. The IR lasers induced heating promotes diffusion of point defects across the structure. These defects enhance intermixing of the well and barrier atoms at elevated temperatures, resulting in increased bandgap energy in the laser treated areas [28,29]. Due to the changing effective dwell time, a graded bandgap material can be created depending on the laser beam size, power and displacement parameters.

2.3. Photoluminescence characterization

In order to measure the results of laser-induced bandgap shifting, the sample was characterized by collecting room-temperature photoluminescence (PL) maps using a Philips PLM-150 mapper. The PL signal was collected from the material excited with an Nd:YAG laser operating at 1064 nm, dispersed by a monochromator and collected by an InGaAs detector array. The spatial and spectral resolutions of the PL mapping were 20 μm and 0.6 nm, respectively. Besides the information concerning bandgap energy gradient profiles, the collected PL maps played an important role in the wafer alignment and SLD fabrication process.

2.4. Superluminescent diodes fabrication

SLD fabrication began by removing the protective SiO_2 cap layers using buffered oxide etch of NH_4F:HF (6:1 solution). The 400 nm sacrificial layer of InP was removed by selective chemical etching for 390 seconds in HCl:H_2O 1:1 solution. A fresh 200 nm PECVD SiO_2 layer was then deposited. A schematic drawing of the SLD microstructure fabricated in this work is shown in Fig. 3. The gain guided devices were defined with 30 μm wide injection lines etched in the SiO_2 cap layer and evenly spaced at 300 μm using standard photolithography and BOE etching. To minimize the lasing effect, the injection lines were tilted by 7.5° from the normal to the crystal (1 1 0) facets. After a standard solvent cleaning (acetone, IPA) and O_2 plasma etching (2 minutes at 100 W) to remove any undesired photoresist traces, the front contact layer (consisting in 70 nm of titanium and 170 nm of gold) was deposited using e-beam evaporation. To ensure good facet quality during the cleaving process and a lower backside resistance, mechanical substrate thinning was performed to reduce the device's thickness down to 150 μm. After a second solvent cleaning to remove impurities coming from the thinning process, back electrical contact layers were deposited (14 nm of gold, 14 nm of germanium, 14 nm of gold, 11 nm of nickel and 200 nm of gold). A RTA step (60 s at 400 °C) was finally carried out to optimize the contact's resistance. The final SLD devices were 3 mm long and 300 μm wide.

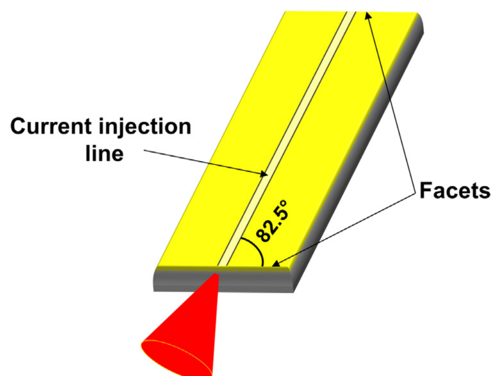

Fig. 3. A schematic of a fabricated SLD device with tilted facets.

2.5. Superluminescent diodes test procedure

The SLD devices were characterized using a Keithley 2520 pulsed current source. Light-intensity characteristics were measured using a Newport 818-IR Germanium photodiode. The pulsed current source was set up with a 1 μs pulse width and a 1 ms pulse delay (0.1% duty cycle). The application of such test parameters was intended to minimize device heating effects at high current density due to the lack of temperature control/dissipation system, while remaining in the operating range of the detector employed in this experiment. We note that similar test parameters were reported in literature discussing the performance of SLD devices [30,31]. SLD output beam was coupled into a 62.5 μm core diameter multi-mode optical fiber and delivered to an Optical Spectrum Analyzer (OSA) Agilent 86140B for spectral properties analysis with tested devices powered in pulsed mode with a 0.5 μs pulse width and a 20 μs pulse delay. SLDs from both bandgap graded and as-grown material were tested.

3. Results and discussion

Fig. 4a shows the PL peak wavelength map of a region of the sample processed under conditions described in the experimental details section. As-grown material shows a PL peak wavelength centered at around 1530 nm (not identified in Fig. 4). After laser annealing, the zone of an intermixed material (blueshifted) is clearly visible with the most intermixed material emitting at near 1410 nm. A 60% decrease of the corresponding PL peak intensity has been observed for the blue shifted region of this material. The primary source of this decrease is the reduced quantum confinement, and related decrease of radiative (electron–hole) recombination in the QWI material. In addition, the PL intensity could be reduced due to increased surface scattering. The Fig. 4b clearly shows the PL peak intensity decrease.

An example of the bandgap gradient achieved in the direction perpendicular to the scan, as indicated by the AB line in Fig. 4a, is plotted in Fig. 5. It can be seen that over a 2 mm distance, the bandgap varies from 1520 nm to 1410 nm between the near as-grown and most blueshifted material.

The region along line AB in Fig. 4a was selected for the fabrication of 3 mm long SLD devices. Due to its reduced optical absorption, the largest bandgap energy material was used for the front (emitting) side of the SLD device.

The light-current (LI) characteristics shown in Fig. 6 compare the emitted electroluminescent (EL) power of SLD devices fabricated from the QWI and from as grown material. The bandgap tuned SLDs exhibit a higher output power for currents below 1.5 A, and a lower output power above this value. This difference between reference and QWI device LI characteristics is linked to their different bandgap energy profile. The QWI induced bandgap energy gradient reduces absorption for photons traveling from rear to front of the fabricated SLD (as they have lower energy compared to blueshifted bandgap). This may promote light emission at low current values and explain the better performance of QWI SLD below 1.5 A injected current. Over this value however, the reference devices output power becomes higher and the power difference increases to be more than two and a half times higher at a 2 A current (4 mW compared to 1.5 mW). This can be related to three phenomena. The most important one is the device amplification efficiency degradation due to the progressive blue

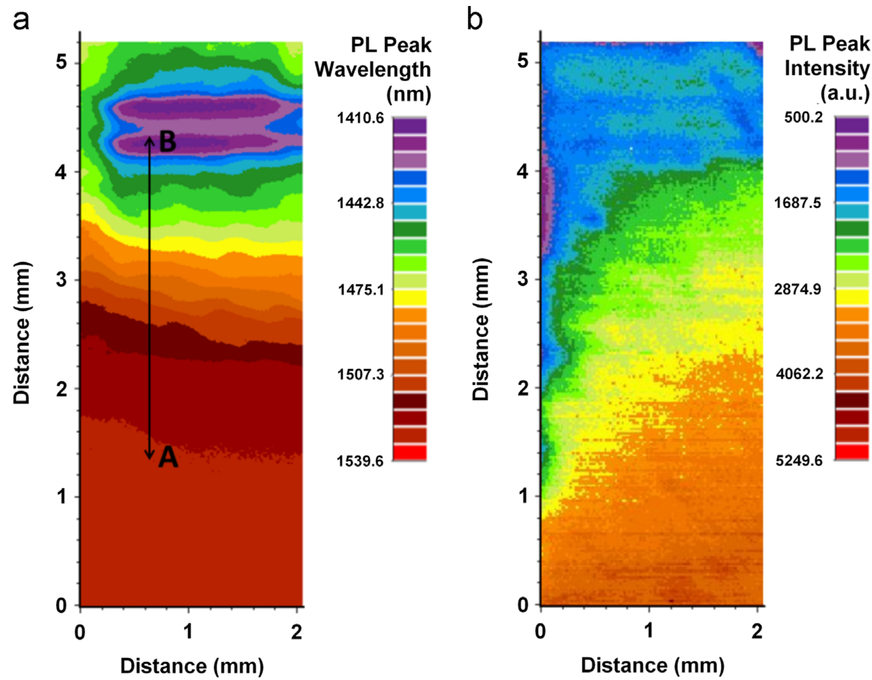

Fig. 4. PL peak wavelength (a) and intensity (b) maps of a sample processed with a dual laser RTA setup.

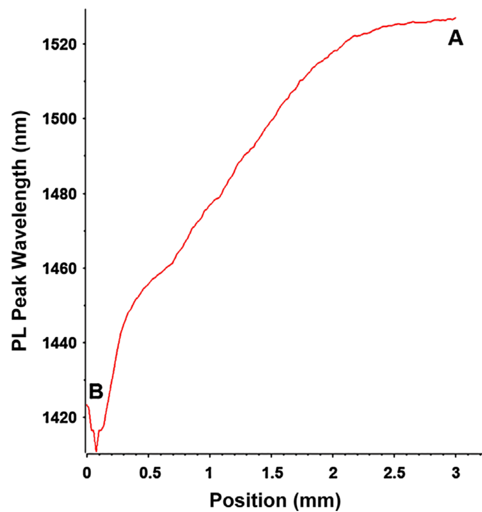

Fig. 5. PL peak wavelength profile along line AB defined in Fig. 4a.

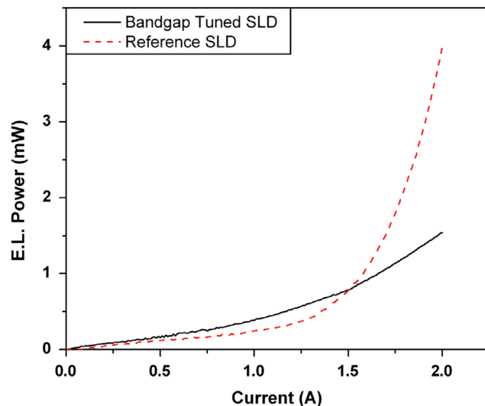

Fig. 6. L-I curves measured under pulsed current of a reference SLD (broken line) and a SLD (solid line) made of the laser processed material.

shift of the material bandgap energy along the waveguiding direction. This quantum well bandgap energy gradient affects gain spectral bandwidth in a similar manner. As a consequence, the rear-to-front traveling light amplification along the device length decreases, since the emitted spectrum of a given region will exhibit a lower energy in comparison to the gain spectrum of the regions closer to the SLD front facet. The two other factors are the reduction of quantum confinement of the intermixed material and possible non-radiative recombination centers created by laser processing. The role of the latter factor was reduced by the combined use of two lasers and by the fast surface scanning of the Nd:YAG laser that allowed to generate weaker temperature gradients and reduced stress during the high power laser exposure of a very limited area of the sample [26]. The fact that QWI SLD shows brighter or equivalent output power for low current density compared to reference SLD tends to validate this hypothesis.

Fig. 7 shows the reference and QWI SLDs output signal spectral evolution for different currents ranging from 1.5 A to 2 A in steps of 0.1 A. As a result of the QWI effect, the 1545 nm peak emission of the as-grown SLD has been blue-shifted to 1445 nm for the intermixed SLD device. The EL intensity for reference devices demonstrates significant spectral ripples for the current exceeding 1.8 A, as some lasing modes become prominent. The spectral ripple amplitude is weaker at this current for the QWI SLD as it emits a weaker signal and the bandgap profile of the device promotes absorption of light propagating in the front-to-rear direction. The spectral FWHM evolution as a function of current for both devices is plotted in Fig. 8 and it demonstrates the broader spectral emission of the QWI SLD device. It ranges from 48 nm at 1.5 A to 46 nm at 2 A, while the reference device varies from 36 nm to 30.5 nm for the same two currents. The significant drop in the spectral width of the reference device is due to the lasing modes appearing for current exceeding 1.8 A.

A comparison of the two devices' spectral properties for an equal emitted power of 0.8 mW (at 1.5 A from Fig. 6) reveals FWHM values of 36 nm and 48 nm for the reference and the intermixed device, respectively. At 1.5 mW, these values change to 35 nm and 46 nm, respectively. This represents a FHWM gain of

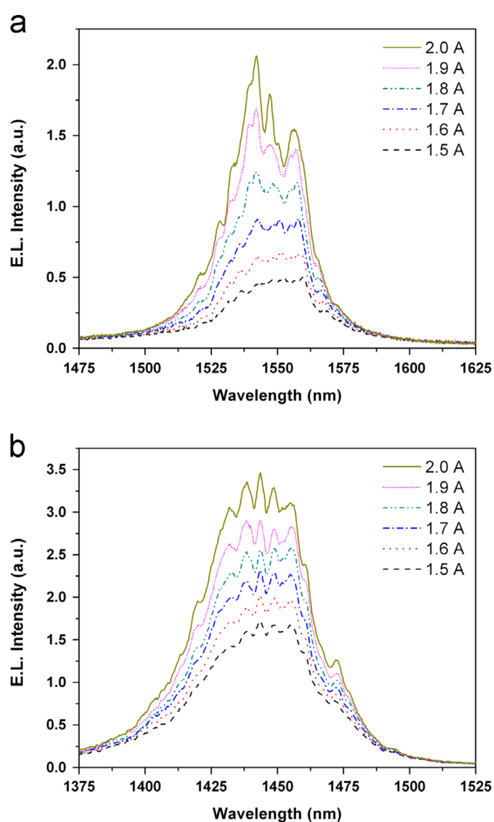

Fig. 7. Spectral evolution of emitted signal for different injected currents of (a) reference SLDs and (b) bandgap tuned SLD devices.

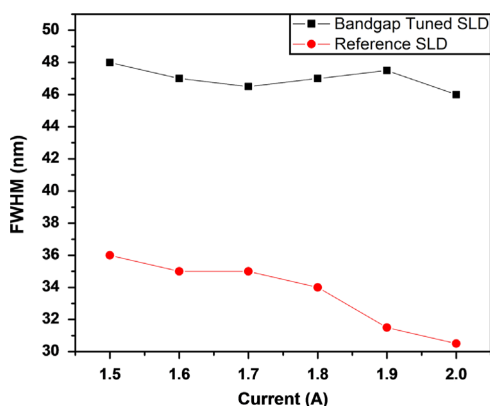

Fig. 8. Comparison of FWHM as a function of injected current between the reference and the bandgap tuned devices.

33% in the first case and 31% in the second one. These results and, in particular, the output power of the QWI SLD device comparable to that of the reference device, indicate the potential of the IR laser QWI technique in delivering multibandgap wafers suitable for the fabrication of SLD devices with attractive parameters. It is relevant to point out that the Laser-QWI technique is well geared towards such a study, including verification of SLD modeling results, due to the ease in generating wafers with different gradient QWI microstructures.

4. Conclusion

We have applied the infrared Laser-RTA technique for bandgap blue-shifting of the InGaAs/InGaAsP/InP QW material designed for SLD devices fabrication. The method combines a 980 nm laser diode, operating at 30 W, with an Nd:YAG laser, operating at 450 mW, for simultaneous heating of the QW material. A controlled speed scanning of the Nd:YAG laser beam along the wafer allowed to fabricate, mask-free, QWI wafers with significant bandgap energy gradient perpendicular to the scan direction. The SLD devices obtained from the QWI material exhibited spectral width emission enhanced by over 33% in comparison to the width of SLD fabricated from the as-grown material, for comparable milliwatt range output power. The fabrication of optimized InGaAs/InGaAsP/InP SLD devices has yet to be carried out, but our results suggest that the IR Laser-RTA technique has the potential to yield QWI material of attractive parameter and quality for cost-effective fabrication of SLD devices. It is difficult to speculate if, at this stage, the Laser-RTA approach is more cost-effective than established epitaxial techniques employed for the fabrication for SLD. However, due to the flexibility of this technique in the fabrication of multibandgap III–V wafers, the Laser-RTA approach could be used for rapid prototyping of SLD and other active/passive devices that otherwise would require complicated (lithography, etching/re-growing) multi-step microfabrication procedures. We have been investigating the Laser-RTA technique for selective area bandgap engineering of III–V quantum semiconductor wafer, but processing of other materials can easily be accommodated.

Acknowledgments

This research was supported by the Natural Sciences and Engineering Research Council of Canada (Discovery Grant no. 122795-2010), the Canada Research Chair in Quantum Semiconductors Program, NanoQuébec and Le Fonds Québécois de la recherche sur la nature et les technologies. Semiconductor wafers, partially subvented by the CMC Microsystems (Kingston, Ontario), were provided by the Canadian Photonics Fabrication Centre (Ottawa, Canada). The authors would like to thank the staff of the Université de Sherbrooke Interdisciplinary Institute for Technological Innovation (3IT) for providing technical support.

References

[1] Fercher AF, Drexler W, Hitzenberger CK, Lasser T. Optical coherence tomography—principles and applications. Reports on Progress in Physics 2003;66 (2):239.
[2] Boehm K, Marten P, Petermann K, Weidel E, Ulrich R. Low-drift fibre gyro using a superluminescent diode. Electronics Letters 1981;17:352.
[3] Kim JH, An SK, Lee SJ, Bae JC, Choi YK, Hong TH. 1.55 μm InGaAsP/InP tapered stripe superluminescent diodes with potential optical sensor system applications. Optics and Laser Technology 2004;36:255–8.
[4] Alphonse GA, Gilbert DB, Harvey MG, Ettenberg M. High-power superluminescent diodes. IEEE Journal of Quantum Electronics 1988;24:2454–7.
[5] Ma H, Chen S, Yi X, Zhu G, Jin J. High power polarization-insensitive 1.3 μm InGaAsP InP quantum-well superluminescent emission diodes grown by MOVPE. Semiconductor Science and Technology 2004;19(7):823.
[6] Nagai H, Noguchi Y, Sudo S. High-power, high-efficiency 1.3 μm superluminescent diode with a buried bent absorbing guide structure. Applied Physics Letters 1989;54(18):1719–21.
[7] Joindot I, Boisrobert CY. Peculiar features of InGaAsP DH superluminescent diodes. IEEE Journal of Quantum Electronics 1989;25(7):1659–65.
[8] Wang CS, Cheng WH, Hwang CJ, Burns W, Moeller R. High power low divergence superradiance diode. Applied Physics Letters 1982;41(7):587–9.
[9] Superlum Diodes, Ltd. 〈http://www.superlumdiodes.com〉; 2013.
[10] Lin CF, Lee BL. Extremely broadband AlGaAs/GaAs superluminescent diodes. Applied Physics Letters 1997;71(12):1598.
[11] Sun ZZ, Ding D, Gong Q, Zhou W, Xu B, Wang ZG. Quantum-dot superluminescent diode: a proposal for an ultra-wide output spectrum. Optical and Quantum Electronics 1999;31(12):1235–46.
[12] Ooi B, Djie H, Wang Y, Tan CL, Hwang J, Fang XM, et al. Quantum dashes on InP substrate for broadband emitter applications. IEEE Journal of Selected Topics in Quantum Electronics 2008;14(4):1230–8.

[13] Jiang Q, Zhang ZY, Hopkinson M, Hogg RA. High performance intermixed p-doped quantum dot superluminescent diodes at 1.2 μm. Electronics Letters 2010;46(4):295–6.
[14] Xin YC, Martinez A, Saiz T, Moscho AJ, Li Y, Nilsen TA, et al. 1.3 μm Quantum-Dot Multisection Superluminescent Diodes With Extremely Broad Bandwidth. IEEE Photonics Technology Letters 2007;19(7):501–3.
[15] Judson P, Groom KM, Childs DTD, Hopkinson M, Hogg RA. Multi-section quantum dot superluminescent diodes for spectral shape engineering. IET Optoelectronics 2009;3(2):100–4.
[16] Li X, Jin P, An Q, Wang Z, Lv X, Wei H, et al. Improved continuous-wave performance of two-section quantum-dot superluminescent diodes by using epi-down mounting process. IEEE Photonics Technology Letters 2012;24(14):1188–90.
[17] Kashima Y, Munakata T. Broad spectrum InGaAsP edge-emitting light-emitting diode using selective-area metal-organic vapor-phase epitaxy. IEEE Photonics Technology Letters 1998;10(9):1223–5.
[18] Ozaki N, Takeuchi K, Ohkouchi S, Ikeda N, Sugimoto Y, Asakawa K, et al. Broadband light source based on four-color self-assembled InAs quantum dot ensembles monolithically grown in selective areas. IEICE Transactions on Electronics 2012;95:247–50.
[19] Ong TK, Yin M, Yu Z, Chan YC, Lam YL. High performance quantum well intermixed superluminescent diodes. Measurement Science and Technology 2004;15(8):1591.
[20] Xu CD, Du GT, Song JF, Huang YZ. Enhancement of the spectral width of high-power 1.5 μm integrated superluminescent light source by quantum well intermixing process. Chinese Physics Letters 2004;21(5):963–5.
[21] Zhou KJ, Jiang Q, Zhang ZY, Chen SM, Liu HY, Lu ZH, et al. Quantum dot selective area intermixing for broadband light sources. Optics Express 2012;20(4):26950–7.
[22] McDougall SD, Kowalski OP, Marsh JH, Aitchison JS. Broad optical bandwidth InGaAs-InAlGaAs light-emitting diodes fabricated using a laser annealing process. IEEE Photonics Technology Letters 1999;11(12):1557–9.
[23] Chia CK, Chua SJ, Dong JR, Teo SL. Ultrawide band quantum dot light emitting device by postfabrication laser annealing. Applied Physics Letters 2007;90(6):061101.
[24] Dubowski JJ, Allen CN, Fafard S. Laser-induced InAs/GaAs quantum dot intermixing. Applied Physics Letters 2000;77(22):3583–5.
[25] Dubowski JJ, Feng Y, Poole P, Buchanan M, Poirier S, Genest J, et al. Monolithic multiple wavelength ridge waveguide laser array fabricated by Nd:YAG laser-induced quantum well intermixing. Journal of Vacuum Science Technology A: Vacuum, Surfaces, and Films 2002;20(4):1426–9.
[26] Stanowski R, Dubowski JJ. Laser rapid thermal annealing of quantum semiconductor wafers: a one step bandgap engineering technique. Applied Physics A: Materials Science and Processing 2009;94:667–74.
[27] Stanowski R, Martin M, Ares R, Dubowski JJ. Iterative bandgap engineering at selected areas of quantum semiconductor wafers. Optics Express 2009;17:19842.
[28] Li EH. Semiconductor Quantum Well Intermixing. Optoelectronic Properties of Semiconductor Series. Gordon & Breach Science Publishers; 2000.
[29] Stanowski R, Voznyy A, Dubowski JJ. Finite element model calculations of temperature profiles in Nd:YAG laser annealed GaAs/AlGaAs quantum well microstructures. Journal of Laser Micro/Nanoengineering 2006;1:1984217–22.
[30] Yamatoya T, Mori S, Koyama F, Iga K. High power GaInAsP/InP strained quantum well superluminescent diode with tapered active region. Japanese Journal of Applied Physics 1999;38(9):5121–2.
[31] Djie HS, Dimas CE, Wang DN, Ooi BS, Hwang JCM, Dang GT, Chang WH. InGaAs/GaAs quantum-dot superluminescent diode for optical sensor and imaging. IEEE Sensors Journal 2007;7(2):251–7.